ACCURACY IMPROVEMENT IN AUTOMATED SURFACE MEASUREMENT

Mushairry Mustaffar
Postgraduate Student *
Deptartment of Civil Engineering and Surveying
University of Newcastle, NSW 2305
AUSTRALIA

Commission III, Working Group III/2

KEY WORDS : digital image matching, surface measurement, object reconstruction, accuracy, surface model

ABSTRACT

Area-based matching has been acknowledged as being more precise than feature-based matching at finding corresponding points on digital images. This paper investigates a method of further improving the accuracy of the area-based technique by modifying the functional model describing the relationship between the windows. The method replaces the approximations made using an affine transformation. It makes use of a surface model and the collinearity conditions in determining the transformation needed. Since there is greater fidelity involved in the transformation, it is hypothesised that the improved functional model will allow the use of larger windows for matching and hence improve accuracy. The derivation of the theory and some experimental results will be presented. Initial experimental results show that the proposed method is capable of attaining absolute accuracy mildly superior to conventional area-based matching.

1.0 INTRODUCTION

Techniques in digital image matching, or image correlation, have been developed within various disciplines over the last few decades and a vast number of approaches exists. These techiques can be classified into two main groups, viz, feature-based and area-based matching. Stereo image matching techniques make use of a selected area or features within the image or the combination of both for matching (Li 1991). However, it is well accepted that area-based matching (ABM) method is more precise than feature-based matching for finding corresponding points on digital images. Methods in area-based matching have been developed by Foerstner (1982) and Gruen (1985). Some examples of the applications and experiments done on ABM in various fields have been reported by Ackermann (1984), Pertl (1985), Rosenholm (1987b), Crippa *et. al.* (1993), Hahn & Brenner (1995). Further extensions of area-based matching were proposed by Gruen & Baltsavias (1987) whereby methods of constraining the matching with model coordinates (X,Y,Z) through the collinearity conditions were proposed. Their methods, known as geometrically constrained area-based matching, use a unified (combined) least squares solution in which corrections to the affine parameters and model coordinates (X,Y,Z) were solved iteratively. Rosenholm (1987a) proposed the method of multi-point area-based matching technique in evaluating three-dimensional models. Area-based method is further extended by Baltsavias (1991) through the use of images from several viewpoints (multi-image). Recent development of the area-based method is proposed by Wrobel (1991), Heipke (1992) whereby matching is done on a global approach by integrating multi-image matching and object surface reconstruction.

This paper investigates a method of improving the accuracy of the traditional area-based technique by modifying the functional model through the use of a surface model to describe the relationship between the windows. The method replaces the assumptions made using an affine transformation. It also serves as a compromise to the more complex global area-based matching method. The method proposed here makes use of a surface model and the collinearity conditions in determining the transformation needed. It solves, through an iterative least squares solution, directly the corrections to image coordinates (x,y) of the search window. In addition, two 'new' unknowns, the gradients in X and Y directions on the surface at the point on the surface which corresponds to the centre of the search window and their second derivatives are introduced. Since the transformation used is more rigorous than the affine, it is hypothesised that the improved functional model will allow the use of larger windows for matching and hence improve accuracy. It is also hypothesised that the use of a better functional model will converge more quickly to give a solution.

2.0 AREA-BASED IMAGE MATCHING USING A SURFACE MODEL

The basic area-based observation equation, which gives a relationship between the radiometric values of corresponding pixels in the left and right image windows, can be written as follows :-

$$I_L(x_L,y_L) + n(x,y) = I_R(x_R,y_R) \quad \ldots (1)$$

where,

- I_L, I_R are the intensities of the left and right pixels respectively
- x_L, y_L are the image coordinates of the left pixel
- x_R, y_R are the corresponding image coordinates on the right image
- $n(x,y)$ is the difference caused by noise at the point (x,y) on the left image

* Currently on study leave from :
The Faculty of Civil Engineering
Universiti Teknologi Malaysia
80990 Johor Bahru, MALAYSIA.

The relationship between image coordinates on the left (x_L,y_L) and (x_R,y_R) on the right is given by assuming an affine transformation exists between the windows (Foerstner, 1982). Furthermore, no information of the object is taken into account in the matching process. Matching is solely based on the intensity values of the pixels and the assumed affine transformation. However, if the collinearity conditions were to be used, the transformation could take into consideration the shape of the object. If some information about the object's surface is availabale, then a sensible surface model can be introduced and the model could be improved. This would then constrained the matching to the surface model. In doing so, image coordinates (x_R,y_R) are expressed in terms of (x_L,y_L) using coordinates (X,Y,Z) on the object surface.

Consider a window of size n × n pixels (where n is odd) on the left image with its centre (i.e. the central point) having the coordinates of (x_L,y_L). It should be noted that, 'central point' does not have to be the centre of the window. The term is chosen merely for the convenience of explanation. By using an appropriate surface model, the corresponding position on the right image (x_R,y_R), where x_R,y_R are not neccessarily integers, can be in terms of the central point on the left (x_L,y_L) and the corresponding coordinates (X,Y,Z) on the surface. In addition to the central point, the relationships of neighbouring points, say, $(x_L+\Delta x_L,\ y_L+\Delta y_L)$ on the left image and $(x_R+\Delta x_R,\ y_R+\Delta y_R)$ are also needed. Values Δx_L and Δy_L are known while Δx_R and Δy_R are not known but are defined by the relevant transformation between the windows.

Use of the collinearity equations, would introduce three additional parameters, (X,Y,Z) for the central point and also for each of the neighbouring points. Supposing that the six relative orientation parameters are known, then a relationship can be established that relates (x_L,y_L) to (X,Y,Z). By adopting a suitable surface model coordinates of neighbouring points on the surface can be related to the central point and the replacement of the affine transformation is achieved.

2.1 Functional Model

The coordinates (x_{L_o},y_{L_o}) of the central point, O, of the window on the left image can be represented by :-

$$x_L = f_{x_L}(X_o,Y_o,Z_o) \quad ; \quad y_L = f_{y_L}(X_o,Y_o,Z_o) \qquad \text{... (ii)}$$

where, x_L and y_L are known; (X_o,Y_o,Z_o) are not known (but needed) and an initial estimation can be obtained; f_{x_L} and f_{y_L} are the collinearity conditions. For a neighbouring point, P, with shifts $(\Delta x_L,\Delta y_L)$ from the origin on the left image, then its coordinates can be represented by :-

$$\begin{aligned} x_L+\Delta x_L &= f_{x_L}(X_P,Y_P,Z_P) \\ y_L+\Delta y_L &= f_{y_L}(X_P,Y_P,Z_P) \end{aligned} \qquad \text{... (iii)}$$

where X_P,Y_P,Z_P are the coordinates of the neighbouring points on the surface. If the corresponding shifts on the object are ΔX, ΔY and ΔZ, then eqn (iii) can be written as :-

$$\begin{aligned} x_L+\Delta x_L &= f_{x_L}(X_o+\Delta X,Y_o+\Delta Y,Z_o+\Delta Z) \\ y_L+\Delta y_L &= f_{y_L}(X_o+\Delta X,Y_o+\Delta Y,Z_o+\Delta Z) \end{aligned} \qquad \text{... (iv)}$$

Supposing that matching is to be done for a flat surface then a surface model can now be introduced across the window to represent the surface. This is given by (considering only the first order terms, i.e., a planar surface model) :-

$$\Delta Z = \frac{\partial Z}{\partial X}\Delta X + \frac{\partial Z}{\partial Y}\Delta Y \qquad \text{... (v)}$$

where $(\partial Z/\partial X)$ and $(\partial Z/\partial Y)$ are the gradients of Z in the X and Y directions respectively. These gradients define the model surface and they are to be evaluated in the solution. In turn, the terms ΔX and ΔY can now be expressed in terms of $\Delta x_L,\Delta y_L$:-

$$\Delta X = \frac{\partial X}{\partial x_L}\Delta x_L + \frac{\partial X}{\partial y_L}\Delta y_L \qquad \text{... (vi)a}$$

$$\Delta Y = \frac{\partial Y}{\partial x_L}\Delta x_L + \frac{\partial Y}{\partial y_L}\Delta y_L \qquad \text{... (vi)b}$$

where $(\partial X/\partial x_L)$, $(\partial X/\partial y_L)$, $(\partial Y/\partial x_L)$, $(\partial Y/\partial y_L)$ are derived from the collinearity equations and Δx_L & Δy_L are known shifts on the left image. By substituting eqns (vi)a and (vi)b into eqn(v), ΔZ can be expressed as a function of the shifts $\Delta x_L,\Delta y_L$:-

$$\Delta Z = \frac{\partial Z}{\partial X}\left[\frac{\partial X}{\partial x_L}\Delta x_L + \frac{\partial X}{\partial y_L}\Delta y_L\right] + \frac{\partial Z}{\partial Y}\left[\frac{\partial Y}{\partial x_L}\Delta x_L + \frac{\partial Y}{\partial y_L}\Delta y_L\right] \qquad \text{... (vii)}$$

This implies that ΔX, ΔY and ΔZ can be written in terms of the known shifts Δx_L and Δy_L, as well as the surface gradient $(\partial Z/\partial X)$ and $(\partial Z/\partial Y)$. Since ΔX, ΔY,ΔZ, $(\partial Z/\partial X)$ and $(\partial Z/\partial Y)$ represent the planar surface model of the object, these terms are therefore common to both the left and right windows. In other words, given a neighbouring point on the left image whose are $(x_L+\Delta x_L,\ y_L+\Delta y_L)$, its corresponding coordinates on the right $(x_R+\Delta x_R,\ y_R+\Delta y_R)$ can be estimated via the planar surface model. Thus eqn (i) can now be expanded to represent neighbouring points by :-

$$I_L(x_L+\Delta x_L,y_L+\Delta y_L) + n(x+\Delta x_L,y+\Delta y_L) = I_R(x_R+\Delta x_R,y_R+\Delta y_R) \qquad \text{... (viii)}$$

Linearising eqn(viii) in x_R, y_R, Δx_R and Δy_R will yield :-

$$I_L(x_L+\Delta x_L,y_L+\Delta y_L) + n(x+\Delta x_L,y+\Delta y_L) = I_R^{\,o}(x_R^{\,o}+\Delta x_R^{\,o},y_R^{\,o}+\Delta y_R^{\,o}) + \left[\frac{\partial I_R}{\partial x_R}\right]dx_R + \left[\frac{\partial I_R}{\partial y_R}\right]dy_R + \left[\frac{\partial I_R}{\partial x_R}\right]d\Delta x_R + \left[\frac{\partial I_R}{\partial y_R}\right]d\Delta y_R \qquad \text{... (ix)}$$

where the superscript ^{o} indicates *a priori* estimate and dx_R, dy_R, $d\Delta x_R$ and $d\Delta y_R$ are the corrections to the a priori value. Estimates of x_R^o and y_R^o can be obtained from a suitable method, such as feature detection or even manual selection, and estimates of Δx_R^o and Δy_R^o are computed using provisional values of X_o, Y_o, Z_o, $(\partial Z/\partial X)$, $(\partial Z/\partial Y)$ and the planar surface model. The terms $\partial I_R/\partial x_R$ are $\partial I_R/\partial y_R$ the gradients of the intensities in the x and y directions across the right image.

Looking at eqn (ix), it should be noted that corrections dx_R and dy_R are the terms that are sought in the solution. In order to use the surface model in the matching process, a relationship for the terms $d\Delta x_R$ and $d\Delta y_R$ is needed. Consider the term Δx_R, which can be expressed as :-

$$\Delta x_R = (\partial x_R/\partial X)\Delta X + (\partial x_R/\partial Y)\Delta Y + (\partial x_R/\partial Z)\Delta Z \qquad \text{... (x)}$$

Substituting eqns (vi)a, (vi)b and (vii) into eqn (x) and replacing $(\partial Z/\partial X)$ and $(\partial Z/\partial Y)$ by G and H respectively will give :-

$$\begin{aligned}\Delta x_R = &\left[\frac{\partial x_R}{\partial X}\cdot\frac{\partial X}{\partial x_L}+\frac{\partial x_R}{\partial Y}\cdot\frac{\partial Y}{\partial x_L}\right]\Delta x_L+\left[\frac{\partial x_R}{\partial X}\cdot\frac{\partial X}{\partial y_L}+\frac{\partial x_R}{\partial Y}\cdot\frac{\partial Y}{\partial y_L}\right]\Delta y_L\\ &+\left[\frac{\partial x_R}{\partial Z}\cdot\frac{\partial X}{\partial x_L}\Delta x_L+\frac{\partial x_R}{\partial Z}\cdot\frac{\partial X}{\partial y_L}\Delta y_L\right]G\\ &+\left[\frac{\partial x_R}{\partial Z}\cdot\frac{\partial Y}{\partial x_L}\Delta x_L+\frac{\partial x_R}{\partial Z}\cdot\frac{\partial Y}{\partial y_L}\Delta y_L\right]H \qquad \text{... (xi)}\end{aligned}$$

Equation (xi) expresses Δx_R in terms of the known shifts Δx_L , Δy_L on the left image, the partial derivatives of the collinearity equations (calculated using provisional values of x_R^o, y_R^o and computed X_o, Y_o, Z_o) and the terms G, H as obtained from the planar surface model. As such, only G and H are not known and to be solved, hence :-

$$d\Delta x_R = \frac{\partial \Delta x_R}{\partial G}dG+\frac{\partial \Delta x_R}{\partial H}dH \qquad \text{... (xii)}$$

The partial derivatives $(\partial \Delta x_R/\partial G)$ and $(\partial \Delta x_R/\partial H)$ are obtainable from eqn(xi), which are :-

$$\frac{\partial \Delta x_R}{\partial G} = \left[\frac{\partial x_R}{\partial Z}\cdot\frac{\partial X}{\partial x_L}\Delta x_L+\frac{\partial x_R}{\partial Z}\cdot\frac{\partial X}{\partial y_L}\Delta y_L\right] \qquad \text{... (xiii)a}$$

$$\frac{\partial \Delta x_R}{\partial H} = \left[\frac{\partial x_R}{\partial Z}\cdot\frac{\partial Y}{\partial x_L}\Delta x_L+\frac{\partial x_R}{\partial Z}\cdot\frac{\partial Y}{\partial y_L}\Delta y_L\right] \qquad \text{... (xiii)b}$$

Similarly, the relationships for Δy_R and $d\Delta y_R$ are :-

$$\begin{aligned}\Delta y_R = &\left[\frac{\partial y_R}{\partial X}\cdot\frac{\partial X}{\partial x_L}+\frac{\partial y_R}{\partial Y}\cdot\frac{\partial Y}{\partial x_L}\right]\Delta x_L+\left[\frac{\partial y_R}{\partial X}\cdot\frac{\partial X}{\partial y_L}+\frac{\partial y_R}{\partial Y}\cdot\frac{\partial Y}{\partial y_L}\right]\Delta y_L\\ &+\left[\frac{\partial y_R}{\partial Z}\cdot\frac{\partial X}{\partial x_L}\Delta x_L+\frac{\partial y_R}{\partial Z}\cdot\frac{\partial X}{\partial y_L}\Delta y_L\right]G\\ &+\left[\frac{\partial y_R}{\partial Z}\cdot\frac{\partial Y}{\partial x_L}\Delta x_L+\frac{\partial y_R}{\partial Z}\cdot\frac{\partial Y}{\partial y_L}\Delta y_L\right]H \qquad \text{... (xiv)}\end{aligned}$$

while, the partial derivatives are given by :-

$$\frac{\partial \Delta y_R}{\partial G} = \left[\frac{\partial y_R}{\partial Z}\cdot\frac{\partial X}{\partial x_L}\Delta x_L+\frac{\partial y_R}{\partial Z}\cdot\frac{\partial X}{\partial y_L}\Delta y_L\right] \qquad \text{... (xv)a}$$

$$\frac{\partial \Delta y_R}{\partial H} = \left[\frac{\partial y_R}{\partial Z}\cdot\frac{\partial Y}{\partial x_L}\Delta x_L+\frac{\partial y_R}{\partial Z}\cdot\frac{\partial Y}{\partial y_L}\Delta y_L\right] \qquad \text{... (xv)b}$$

Partial derivatives $(\partial x_R/\partial X_o)$, $(\partial y_R/\partial X_o)$, $(\partial x_R/\partial Y_o)$, $(\partial y_R/\partial Y_o)$, $(\partial x_R/\partial Z_o)$ and $(\partial y_R/\partial Z_o)$ can be obtained from the collinearity equation and their form is well documented in most photogrammetric books.

Substituting eqns(xiii) and (xv) into the eqn (ix), the linearised observation equation would be :-

$$\begin{aligned}&I_L(x_L+\Delta x_L, y_L+\Delta y_L) + n(x+\Delta x_L, y+\Delta y_L) =\\ &\quad I_R^o(x_R^o+\Delta x_R^o, y_R^o+\Delta y_R^o)\\ &\quad +\left[\frac{\partial I_R}{\partial x_R}\right]dx_R+\left[\frac{\partial I_R}{\partial y_R}\right]dy_R\\ &\quad +\left[\frac{\partial I_R}{\partial x_R}\cdot\frac{\partial \Delta x_R}{\partial G}+\frac{\partial I_R}{\partial y_R}\cdot\frac{\partial \Delta y_R}{\partial G}\right]dG\\ &\quad +\left[\frac{\partial I_R}{\partial x_R}\cdot\frac{\partial \Delta x_R}{\partial H}+\frac{\partial I_R}{\partial y_R}\cdot\frac{\partial \Delta y_R}{\partial H}\right]dH \qquad \text{... (xvi)}\end{aligned}$$

Equation (xvi) is non-linear in dx_R, dy_R, dG and dH, thus an iterative least squares solution is needed to solved for the corrections.

2.2 Computational Steps

The steps needed in evaluating the coefficients can be summarised as follows :-

(a) Select a window of n × n pixels in the left image and let the coordinates of the central point be (x_L, y_L). The initial estimate of corresponding position of the central point (x_R, y_R) is then obtained.

(b) Using these coordinates and the relative orientation parameters, the corresponding (provisional) object coordinates, X_o, Y_o, Z_o, are computed.

(c) Determine the shift Δx_L and Δy_L so as to represent the position of a neighbouring point with respect to (x_L, y_L). This is followed by computing the partial derivatives for the planar surface model and subsequently ΔX, ΔY and ΔZ, as shown in eqns (vi)a, (vi)b and (vii), are evaluated at this position.

(d) With the information obtained in (c) the values of Δx_R and Δy_R are calculated using eqns (xi) and (xiv), thus yielding the corresponding coordinates of x_L',y_L' on the right image, i.e. x_R', y_R'.

(e) The values of x_R', y_R' obtained in (d) would enable the computation of the partial derivatives $\partial x_R/\partial X$, $\partial y_R/\partial X$, $\partial y_R/\partial X$, $\partial y_R/\partial Y$, $\partial x_R/\partial Z$ and

$\partial y_R/\partial Z$ which constitute the coefficients of the linearised observation equation.

(f) The intensity values at x_L', y_L' and x_R', y_R' are obtained and the gradients $\partial I_R/\partial x_R$ and $\partial I_R/\partial y_R$ are computed.

(g) Steps (c) to (f) are repeated for every pair in the windows, and thus, a set of observation equations (eqn(xvi)) is formed.

2.3 Radiometric Parameters

So far, the observation equation (eqn(xvi)) only models the geometrical relationship between the corresponding pixels in both images. Introducing radiometric parameters r_1 and r_2 (Pertl 1985), which are an absolute difference and a contrast, to model the radiometric differences between the two images, then eqn (viii) will take the following form :-

$$I_L(x_L+\Delta x_L, y_L+\Delta y_L) + n(x+\Delta x_L, y+\Delta y_L) = r_1 + r_2 I_R(x_R+\Delta x_R, y_R+\Delta y_R) \quad \text{... (xvii)}$$

and linearising would yield :-

$$I_L(x_L+\Delta x_L, y_L+\Delta y_L) + n(x+\Delta x_L, y+\Delta y_L) = r_1^o + r_2^o I_R^o(x_R^o+\Delta x_R^o, y_R^o+\Delta y_R^o) + dr_1 + \{I_R^o(x_R^o+\Delta x_R^o, y_R^o+\Delta y_R^o)\}\, dr_2 + \left[\frac{\partial I_R}{\partial x_R}\right] r_2^o dx_R + \left[\frac{\partial I_R}{\partial y_R}\right] r_2^o dy_R + \left[\frac{\partial I_R}{\partial x_R}\cdot\frac{\partial \Delta x_R}{\partial G} + \frac{\partial I_R}{\partial y_R}\cdot\frac{\partial \Delta y_R}{\partial G}\right] r_2^o dG + \left[\frac{\partial I_R}{\partial x_R}\cdot\frac{\partial \Delta x_R}{\partial H} + \frac{\partial I_R}{\partial y_R}\cdot\frac{\partial \Delta y_R}{\partial H}\right] r_2^o dH \quad \text{... (xviii)}$$

where r_1^o, r_2^o are the *a priori* estimates of the radiometric parameters and dr_1, dr_2 are the corrections to the a priori value. The solution is solved iteratively until a suitable stopping criteria is met. In the initial iteration, the values of r_1^o and r_2^o are 0 and 1 respectively.

2.4 Higher Order Surface Model

When dealing with complex shapes, eqn (xviii) can be extended to include second or higher order terms. For instance, if a second order model were used, then eqn (xviii) would contain the terms dG^2, dH^2 and dGH. The least squares solution would then has to solve for these three additional unknowns.

3. EXPERIMENTS USING OBJECTS OF KNOWN DIMENSIONS

Tests of the method were carried out using images of both a 6 mm thick aluminium plate and a PVC cylinder. These objects were chosen because they are smooth and of known dimension. Hence, results obtained could be easily verified with known quantities. Images were taken using a pair of Philips CCD sensors fitted with 25 mm f1.4 Fujinon lenses. These images were then captured by a PC Vision Plus A/D frame grabber. A scale factor exists in the x direction (1 : 1.18) as sizes of image sampled and grabbed are different. These cameras are mounted in a box, with a base distance of approximately 160 mm. The relative orientations of these cameras are known. A projector was fitted in between the lenses for the purpose of projecting patterns onto the object. The pattern used in this investigation was a diamond shaped mesh.

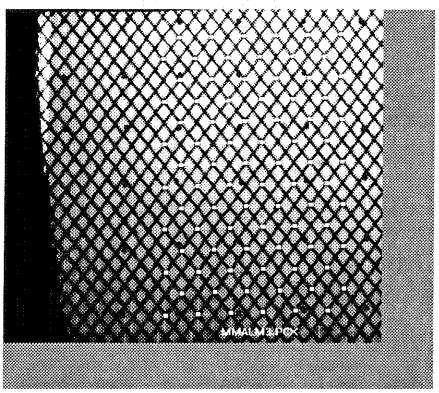

Figure 1a

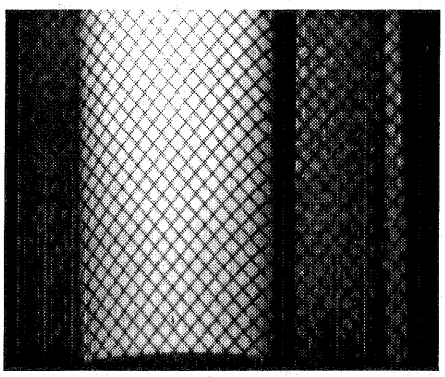

Figure 1b

Figures 1a and 1b show the mesh being projected to the aluminium plate and the cylinder respectively. Points of interest in the image are the intersections of the mesh (nodes). These are determined by digitising manually but efforts are being made to include a 2D epipolar search for this purpose. A total of 66 points and 95 points were selected for matching on the plate and the cylinder respectively. The sizes of windows used in the test range from 9×9 to 101×101 pixels.

In the case of the aluminium plate a first and second order surface model were used, whereas, only a second order surface model was used for the cylinder.

4. ANALYSIS OF RESULTS

Results obtained from the proposed method (hereby referred to as 1SM and 2SM for first order and second order surface respectively) were compared against those obtained form the ABM method. Comparisons were done on the following basis :-

(a) the internal precision, which is indicated by error ellipses computed using the standard errors obtained from the least squares adjustment.

(b) the accuracy, which was obtained by fitting the matched coordinates to a plate (plane) or cylinder.
(c) the computation time

4.1 Error Ellipses

Fig. 2 Axes of error ellipse against window size (aluminium)

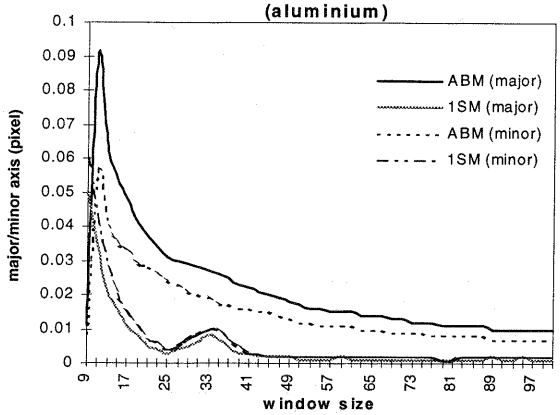

Fig. 3. Axes of the error ellipse against window size (cylinder)

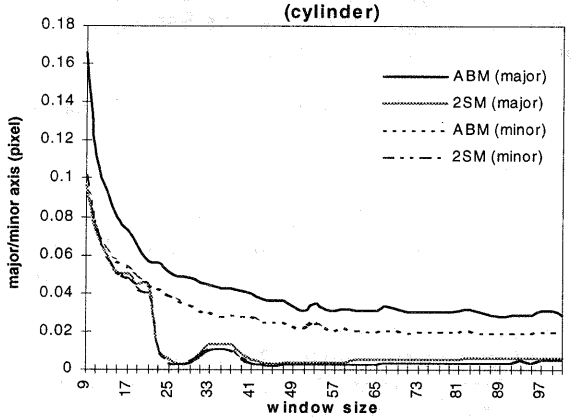

Figures 2 and 3 show the magnitudes of the standard errors, represented by an error ellipse, as plotted against the window size for the aluminium plate and the cylinder respectively. It can be seen that in fig. 2 that the magnitudes of the major and minor axes for the 1SM are always smaller than those from the ABM method. At maximum window size (101 x 101) the difference in major and minor axes is almost 0.01 and 0.02 pixels respectively, in favour of the 1SM method. The results obtained for the cylinder show a similar pattern (fig. 3). The difference between the major and minor axes at maximum window size is about 0.03 and 0.02 pixels respectively. This indicates that the 1SM and 2SM methods are better functional models and are able to model the observations to a better degree than the conventional ABM.

4.2 Test of Accuracy

The accuracy of the matched coordinates obtained was determined by using a surface fitting program. Figures 4 and 5 show the standard errors of the goodness of surface fit in mm for the plate and cylinder respectively.

Fig. 4 Standard error of surface fitting against window size (aluminium)

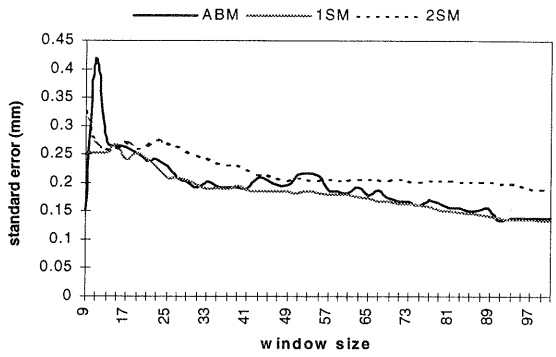

Fig. 5 Standard error of surface fittting against window size (cylinder)

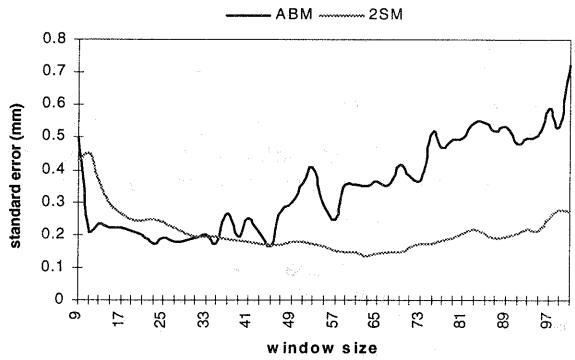

(a) Aluminium plate
As mentioned earlier, both the 1SM and 2SM models were tested on the aluminium plate. Figure 4 shows the three curves representing the standard errors for ABM, 1SM and 2SM. It can be seen that the curve representing the standard errors for the 1SM model is smoother than the curve for ABM. However, the values of the standard error for both methods do not differ greatly. The minimum standard deviation obtained through both the ABM and 1SM methods is approximately 0.15mm.

On the other hand, the standard errors for the 2SM are greater than both the ABM and 1SM methods at any window size. This could indicate the use of unnecessary parameters (curvature) to represent the aluminium plate in the matching process.

(b) Cylinder
To test the accuracy of the method on the cylinder only a 2SM was used. It was decided not to include the 1SM model as it does not contain any curvature to represent the cylinder. Figure 5 shows that the standard errors obtained in using a second order surface model (2SM) to represent the cylinder is significantly smaller compared to ABM at window sizes 35x35 and larger. However, at smaller window sizes, as from 9x9 to 35x35, it seems that the second order terms contributed the problem of overparametrisation. This can be explained by the fact that, for smaller windows sizes, the area to be matched is almost a plane thus introducing

unnecessary terms in the matching process. This therefore would yield less accurate results. The minimum standard deviation for ABM and 2SM are approximately 0.19mm and 0.13mm respectively. This shows that accuracy from the 2SM method is better than the ABM.

4.3 Computation Time

	Computation time (min:sec)	
Window size	ABM	2SM
9 x 9	00:26	00:21
55 X 55	07:38	06:32
101 X 101	34:26	33:51

Table 1. Computation time for the ABM and SM methods

Table 1 compares the computation time of the ABM and SM methods for the cylinder (95 points) at window sizes 9, 55 and 101 pixels. The stopping criteria used for the least squares solution in both methods are :-

(a) rate of convergence (Mikhail & Ackermann, 1976), which is 0.01 pixel
(b) the magnitude of the corrections to the unknowns, which is 0.01 pixel
(c) the maximum number of iterations, which is 16
(d) the detection of unstable/weak normal equations by the Singular Value Decomposition (SVD) method (Griffiths & Hill, 1985).

From Table 1, it can be seen that, the computation time taken for the SM method at any window size is less than those of the ABM. This shows that the proposed functional model has improved, thus, converges more quickly even though it has 9 (as opposed to 8 for the ABM) parameters to solve.

5. DISCUSSION AND CONCLUSIONS

It has been shown that, the internal precision obtained from the 1SM and 2SM methods is much higher than ABM for both the plate and the cylinder. This suggests that the functional model has been improved to fit the observations more closely.

The use of second order parameters in matching plane surfaces and for smaller window sizes has been found to give inaccurate results. This is probably due to overparametrisation. Therefore, surface model should be kept simple (only first order) if surfaces to be measured are plane or working with smaller windows. The accuracy of the matched coordinates from the 1SM and 2SM methods was also shown to be higher than the ABM.

This experiment has shown that the conventional ABM functional model has been improved through the use of a surface model. This is reflected in the attained accuracy , convergence, and computation time. It has also shown that suitable surface models should be used when dealing with different surfaces. Comparisons with more complex ABM methods, such as the geometrically constrained and global matching would be of great interest.

REFERENCES

Ackermann, F., 1984. Digital Image Correlation : Performance and Potential Application in Photogrammetry. Photogrammetric Record, 11(64), pp. 429-439

Baltsavias, E.P., 1991. Multiphoto Geometrically Constrained Matching. Ph.D. thesis, Institute of Geodesy and Photogrammetry. Mitteilungen Nr. 49, 221p

Crippa, B., Forlani, G. & de Haan, A., 1993. Automatic Deformation Measurement from Digital Images. Optical 3-D Measurement Techniques II (ed. Gruen/Kahmen), pp. 557-563

Foerstner, W., 1982 . On the Geometric Precision of Digital Correlation. Proceedings of ISPRS Commission III Symposium, Rovaneimi, Finland, June 7 - 11, 1982. In IAP 24(3), pp. 176-189

Griffiths, P. & Hill, I.D., 1985. Applied Statistics Algorithms. Ellis Horwood Ltd., England, 307p

Gruen, A.W., 1985. Adaptive Least Squares Correlation : A Powerful Image Matching Technique. South African Journal of Photogrammetry, Remote Sensing and Cartography. 14(3), pp. 175-187

Gruen, A.W. & Baltsavias, E.P., 1987. High Precision Image Matching for Digital Terrain Model Generation. Photogrammetria 42(3), pp. 97-102

Hahn, M. & Brenner, C., 1995. Area Based Matching of Colour Images. ISPRS Intercommission Workshop "From Pixels to Sequences", Zurich. 30(Part 5W1), pp. 227-234

Heipke, C., 1992. A Global Approach for Least-Squares Image Matching and Surface Reconstruction in Object Space. Photogrammetry Engineering and Remote Sensing, 58(3), pp. 317-323

Mikhail. E.M. & Ackermann, F., 1976. Observations and Least Squares. Harper & Row, New York, 497p

Pertl, A., 1985. Digital Image Correlation with an Analytical Plotter. Photogrammetria, 40, pp. 9-19

Rosenholm, D., 1987a. Multi-Point Matching Using the Least-Squares Technique for Evaluation of Three-Dimensional Models. Photogrammetric Engineering and Remote Sensing, 53(6), pp. 621-626

Rosenholm, D., 1987b. Least Squares Matching Method : Some Experimental Results. Photogrammetric Record 12(70), pp. 493-512

Wrobel, B.P., 1991. Least-squares Methods for Surface Reconstruction from Images. ISPRS Journal of Photogrammetry and Remote Sensing, 46, pp. 67-84